Supplementary Information File for
Progesterone activates GPR126 to promote breast cancer development via the Gi pathway

Wentao An[a,1], Hui Lin[a,1], Lijuan Ma[b,1], Chao Zhang[b], Yuan Zheng[c], Qiuxia Cheng[a], Chuanshun Ma[d], Xiang Wu[b], Zihao Zhang[a], Yani Zhong[b], Menghui Wang[a], Dongfang He[b], Zhao Yang[b], Lutao Du[e], Shiqing Feng[f,g,h], Chuanxin Wang[e], Fan Yang[a,f], Peng Xiao[b,e,2], Pengju Zhang[b,2], Xiao Yu[a,b,2], and Jin-Peng Sun[b,c,e,f,2]

Affiliations:

[a]Key Laboratory Experimental Teratology of the Ministry of Education, Department of Physiology, School of Basic Medical Sciences, Cheeloo college of Medicine, Shandong University, Jinan, Shandong, 250012, China.

[b]Key Laboratory Experimental Teratology of the Ministry of Education, Department of Biochemistry and Molecular Biology, School of Basic Medical Sciences, Cheeloo College of Medicine, Shandong University, Jinan, Shandong, 250012, China.

[c]Department of Physiology and Pathophysiology, School of Basic Medical Sciences, Peking University, Key Laboratory of Molecular Cardiovascular Science, Ministry of Education, Beijing, 100191, China.

[d]School of Pharmacy, Binzhou Medical University, Yantai, Shandong, 264003, China

[e]Department of Clinical Laboratory, The Second Hospital, Cheeloo College of Medicine, Shandong University, Jinan, 250033, Shandong, China.

[f]Advanced Medical Research Institute, Shandong University, Jinan, China.

[g]Department of Orthopaedics, Qilu Hospital, Cheeloo College of Medicine, Shandong University, Jinan, China.

[h]Shandong University Center for Orthopaedics, Cheeloo College of Medicine, Shandong University, Jinan, China.

[1] These authors contributed equally to this work.

* Corresponding author. Email: sunjinpeng@sdu.edu.cn ;
yuxiao@sdu.edu.cn;
zhpj@sdu.edu.cn
pengxiao@sdu.edu.cn

This supplementary Information File includes:

Materials and Methods

Supplemental Figures 1-12

Supplemental Tables 1-2

Materials and Methods

IHC and Scoring.

Samples of breast tumor and adjacent tissues were obtained from 14 patients undergoing surgical excision of tumors at Shandong Provincial Hospital (Jinan, China). The use of pathological specimens and the review of all pertinent patient records were approved by the Shandong Provincial Hospital Ethical Review Board. Informed consent was obtained from the patients. Frozen tissues were subjected to western blot analysis. Breast tissue microarray was purchased from Wuhan Servicebio Technology, which contain 42 cases of breast adenocarcinoma with paired paraneoplastic tissues. The clinic pathological features of the samples were available on the company's website. Immunohistochemistry was performed on formalin-fixed paraffin-embedded (FFPE) tissue according to standard protocols. After fixation, dehydration, baking, dewaxing and hydration, the slices were repaired with 0.1M sodium citrate, boiled for 30 min, cooled and inactivated with 3% catalase for 20 min. The slices were blocked with 5% bovine serum albumin for 60 min at room temperature and incubated overnight with primary antibodies (1:300, GPR126, Proteintech) in humidified box at 4 °C. Then, the horseradish peroxidase (HRP)-labelled streptavidin protein working solution was added dropwise into the slices at 37°C for 30 min. The slices were stained with diaminobenzidine and counterstained with hematoxylin. After that, the slices were observed using the optical microscope. The score for the proportions of the stained cells was scaled as 0 for no immunohistochemical signal or less than 5%, 1 for 5-25%, 2 for 25-50%, 3 for 50-75%, and 4 for more than 75%. The score for IHC intensity was scaled as 0 for no IHC signal, 1 for weak, 2 for moderate, and 3 for strong IHC signals. For each IHC slide, five high magnification fields (×200 magnification) were randomly selected to take photos. The overall quantitation of IHC score was obtained by multiplying the score of the staining intensity and the score of the fraction of positive cells of five different high-multiplier fields with the maximum score of 12. The scoring results were analyzed by three experienced pathologists.

cAMP Level Detection by ELISA Kit.

MDA-MB-231 cells with stably GPR126 silencing (Sh-GPR126) and their negative control cells (Sh-CTRL) were seeded in 10 cm dishes and cultured for 48h. After starvation in serum-free medium for 12h, cells were then treated with Forskolin (Fsk, 5μM) alone or along with

different concentrations of progesterone (P4, 10 nM) or 17OHP (10 nM) for 10min. Then, cells were washed with pre-cooled PBS for three times and further re-suspended in 0.1 N HCl containing 500 μM IBMX at a 1:5 ration (w/v) for 10 min at room temperature with gentle mixing. Samples were then neutralized with 1N NaOH at a 1:10 (v/v) ratio. Insoluble cellular debris were removed by centrifugation at 600 g for 10 minutes at 4°C. Supernatants were then prepared for cAMP determination using the cAMP Parameter Assay Kit (R&D Systems) according to the manufacturer's instruction.

Cell Proliferation Assay.

GPR126 stably silencing MDA-MB-231 cells (sh-GPR126-1 and sh-GPR126-2) and their negative control cells (sh-CTRL) were seeded in 96-well plates at a density of 2,000 cells per well. Then, the cells were treated with progesterone (10 nM) alone or together with SRC-I1 (2 μM) or PTX (100 ng/mL) for 72 h. Cell proliferation was analyzed using 3-(4,5-dimethylthiazol-2-yl)-2, 5-diphenyltetrazolium bromide (MTT) assay. In brief, 10 μl MTT (5mg/mL, Sigma Aldrich) was added into each well for 4 h after which particles were dissolved using DMSO. Absorbance of the solution was measured at 492 nm on a microplate reader.

Colony Formation Assays.

GPR126 stably silencing MDA-MB-231 cells (sh-GPR126-1 and sh-GPR126-2) and their negative control cells (sh-CTRL) were seeded in 6-well plate at a density of 800 cells per well in complete medium. Then, cells were treated with progesterone (10 nM) or DMSO for ten days. During culture process, medium were refreshed every 3 days. Cells were fixed with 4% paraformaldehyde for 15 min at room temperature and then washed with PBS for 3 times. Next, cells were stained with Giemsa (Solarbio, China) for 15 min. The cells were washed with PBS and visible colonies were counted. Colony numbers were calculated and analyzed using GraphPad Prism 7.0. The experiments were repeated three times.

Nude Mice Xenograft Model.

Nude female mice (5 weeks old) were purchased from Beijing Laboratory Animal Co.Ltd., and maintained in micro-isolator cages. All animals were used in accordance with institutional guidelines and the current experiments were approved by the Use Committee for Animal Care of Shandong University. For establishment of Xenograft model, the nude mice were randomly divided into two groups (n=12). GPR126 stable silencing cells (shGPR126, 2×10^6) and their

control cells (sh-CTRL, 2×10^6) were respectively, injected subcutaneously into the axilla of each nude mouse. The mice inoculated with sh-GPR126 or sh-CTRL cells were divided randomly into the following two groups that received either vehicle control (DMSO) or 15 mg/kg progesterone (n=6 per group) intraperitoneally every three days for thirty days. Serum progesterone levels were detected using ELISA Kit (Jiangsu Meimian industrial Co., Ltd) at different time points after progesterone injection. The body weight and tumor diameters were measured every 2 days. Tumor growth was plotted as tumor volume versus time. The tumor volume was calculated by the formula (length) × (width^2)/2. After 32 days, the nude mice were sacrificed and tumors were excised and weighed.

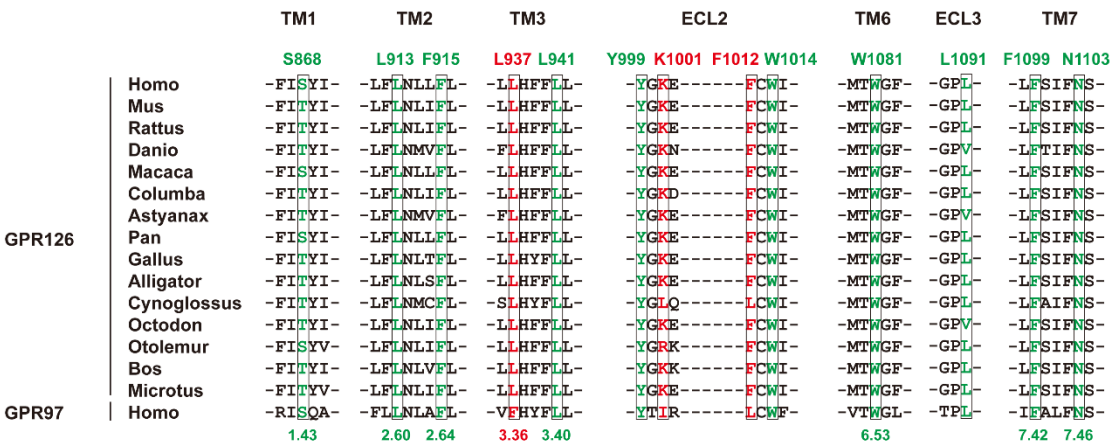

Supplemental Figure 1. Sequence alignment of residues involved in binding pocket in GPR126 from the indicated different species with those interacting with glucocorticoids in human GPR97 located in TM1, TM2, TM3, ECL2, TM6, ECL3 and TM7. The $L^{3.36}$, $K1001^{ECL2}$, $F1012^{ECL2}$ motifs of GPR126 receptors are highlighted in red, whereas the $S^{1.43}$, $L^{2.60}$, $L^{2.64}$, $L^{3.40}$, $Y999^{ECL2}$, $W1014^{ECL2}$, $W^{6.53}$, $L1091^{ECL3}$, $F^{7.42}$ and $N^{7.46}$ pairs are highlighted in green.

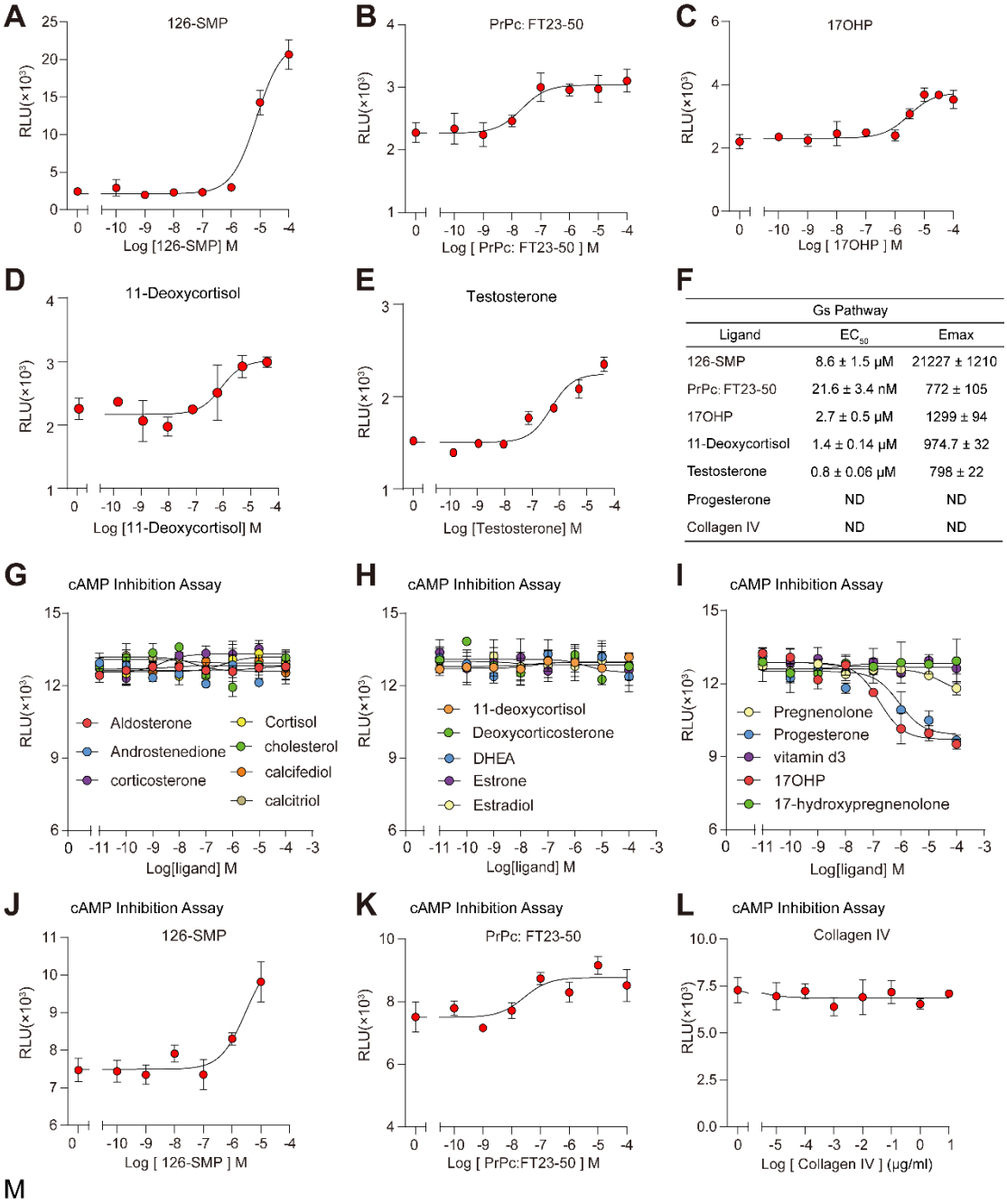

Gs Pathway		
Ligand	EC_{50}	Emax
126-SMP	8.6 ± 1.5 μM	21227 ± 1210
PrPc: FT23-50	21.6 ± 3.4 nM	772 ± 105
17OHP	2.7 ± 0.5 μM	1299 ± 94
11-Deoxycortisol	1.4 ± 0.14 μM	974.7 ± 32
Testosterone	0.8 ± 0.06 μM	798 ± 22
Progesterone	ND	ND
Collagen IV	ND	ND

M

Gi Pathway		
Ligand	EC_{50}	Emax
126-SMP	ND	ND
PrPc: FT23-50	ND	ND
17OHP	95 ± 1.8 nM	2282 ± 212
Progesterone	539.6 ± 3.1 nM	1882 ± 215
Collagen IV	ND	ND

Supplemental Figure 2. Screening steroids hormones ligands of GPR126

A-E. Concentration-dependent curves of GPR126 stimulated with *Stachel* mimicking peptide (126-SMP) (A), PrPc: FT23-50 (B), 17OHP (C), 11-Deoxycortisol (D) and Testosterone (E) on

intracellular cAMP accumulation.

F. EC_{50} and Emax of curves in A-E were collected and presented in this table.

G-L. Representative dose-response curve of the thirty four steroid ligands as well as *Stachel* mimicking peptide (126-SMP) (J), PrPc: FT23-50 (K) and Collagen IV (L) induced cAMP inhibition in HEK293 cells over-expressing wild-type GPR126 using GloSensor assay.

M. EC_{50} and Emax of curves in G-L were collected and presented in this table.

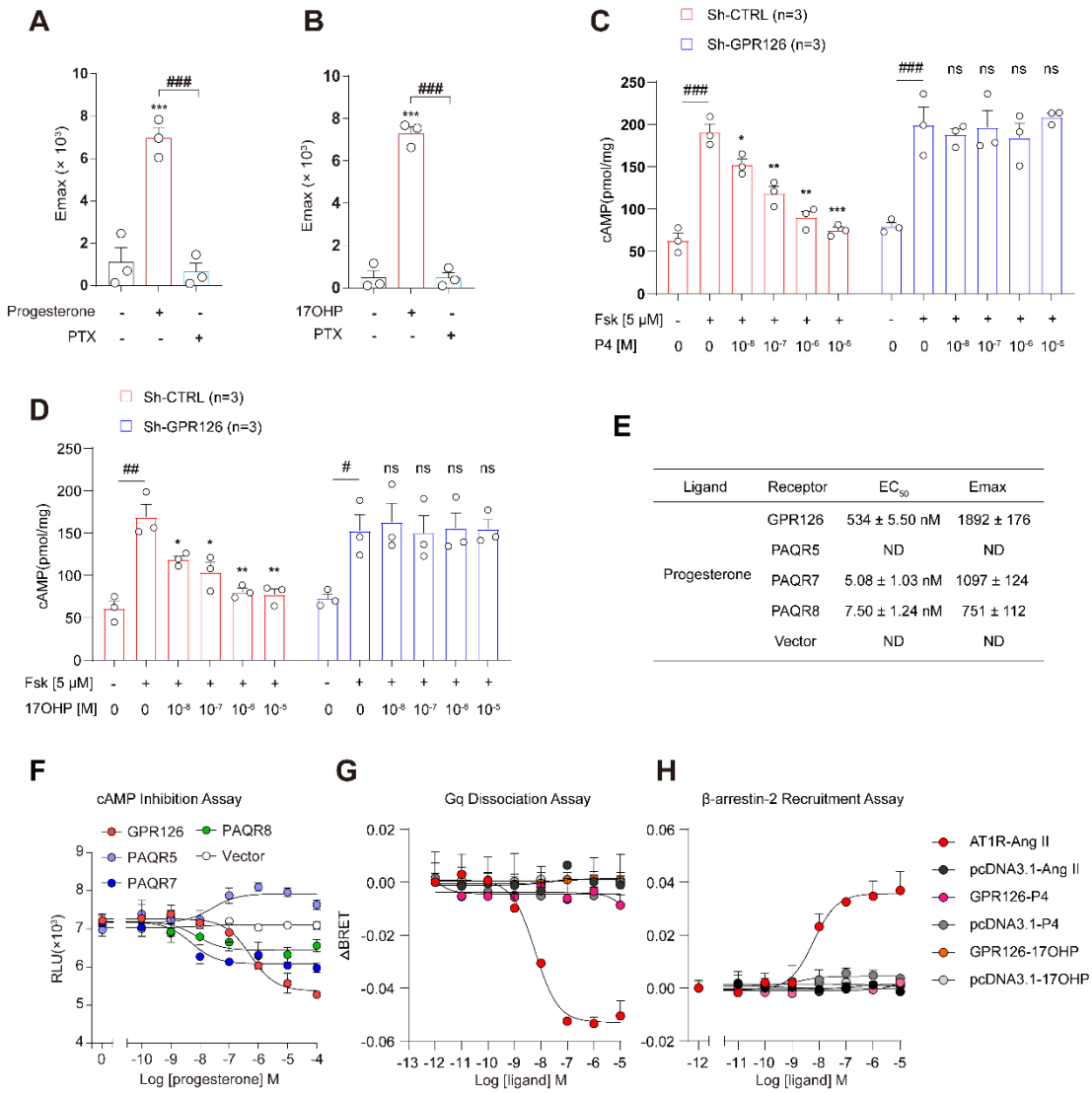

Supplemental Figure 3. Progesterone and 17OHP activates GPR126 via Gi signaling

A-B. The effects of PTX on progesterone (A) or 17OHP (B)-induced Gi activation through GPR126 by calculating their Emax values in GPR126 overexpressing cells of curves stimulated with progesterone or 17OHP alone or together with PTX (100 ng/mL). Values treated with progesterone alone were compared to vehicle. Values treated with progesterone or 17OHP along with PTX were compared to values treated with progesterone or 17OHP alone. The data were represented as the mean ± SEM from three independent experiments and Student's test was used for comparisons between two groups. *** $p < 0.001$, ### $p < 0.001$.

C-D. MDA-MB-231 cells with stably GPR126 silencing (Sh-GPR126) and their negative control cells (sh-CTRL) were treated with Forsklin (Fsk, 5 μM) alone or along with different

concentrations of progesterone (P4) (C) or 17OHP (D) for 10min. Intracellular cAMP levels were then detected using ELISA Kit. The data were represented as the mean ± SEM from three independent experiments and Student's test was used for comparisons between two groups. Data in cells treated with Fsk only were compared to data in cells treated with vehicle in Sh-GPR126 cells or Sh-CTRL cells. ns, not significant, # $p < 0.05$, ## $p < 0.01$, ### $p < 0.001$. Data in cells treated with progesterone (P4) or 17OHP and Fsk were compared to data in cells treated with Fsk in Sh-GPR126 cells or Sh-CTRL cells. ns, not significant, * $p < 0.05$, ** $p < 0.01$, *** $p < 0.001$.

E-F: Representative dose-response curves of progesterone induced cAMP inhibition in HEK293 cells over-expressing GPR126, PAQR5/7/8 or control vehicle (vector), with similar protein expression levels, using GloSensor assay (F). Values are shown as the mean ± SEM of three experiments (n=3) performed in triplicate. EC_{50} and Emax of curves in F were collected in table (E).

G. BRET-based G protein trimer dissociation assays were used to determine the effects of progesterone on Gq coupling of GPR126. AT1R and angiotensin II (Ang II) was set as controls.

H. BRET-based β-arrestin-2 recruitment assays were used to determine the effects of progesterone on β-arrestin-2 recruitment of GPR126. AT1R and angiotensin II (Ang II) was set as controls.

A

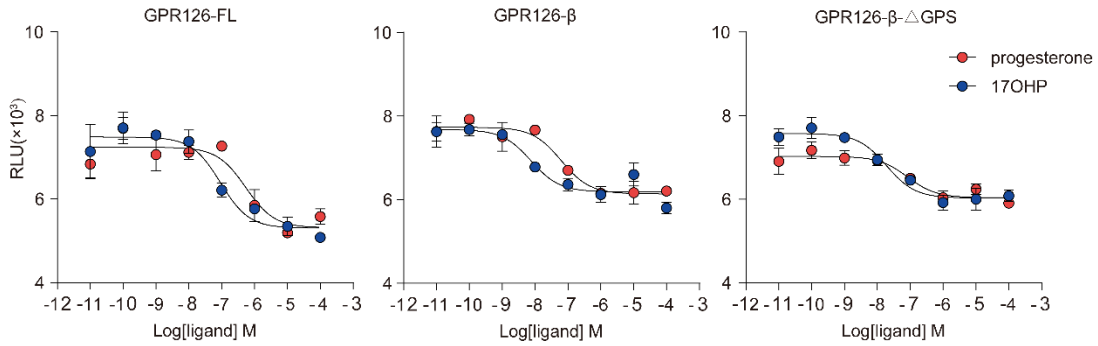

B

		GPR126-FL	GPR126-β	GPR126-β-△GPS
Progesterone	EC_{50}	537 ± 2.55 nM	62 ± 3.21 nM	83 ± 4.10 nM
	Emax	1926 ± 33	1596 ± 120	988 ± 100
17OHP	EC_{50}	94 ± 0.63 nM	10 ± 1.23 nM	19 ± 0.50 nM
	Emax	2181 ± 97	1492 ± 56	1445 ± 110

Supplemental Figure 4. Effects of the α subunit or the *Stachel* sequence of GPR126 on progesterone or 17OHP -induced GPR126 activation

A. Representative dose-response curves of progesterone and 17OHP induced cAMP inhibition in HEK293 cells over-expressing GPR126-FL (left panel), GPR126-β (middle panel) or GPR126-β-ΔGPS (right panel) using GloSensor assay.

B. Summarized EC_{50} and Emax value of progesterone and 17OHP according to the data generated in A.

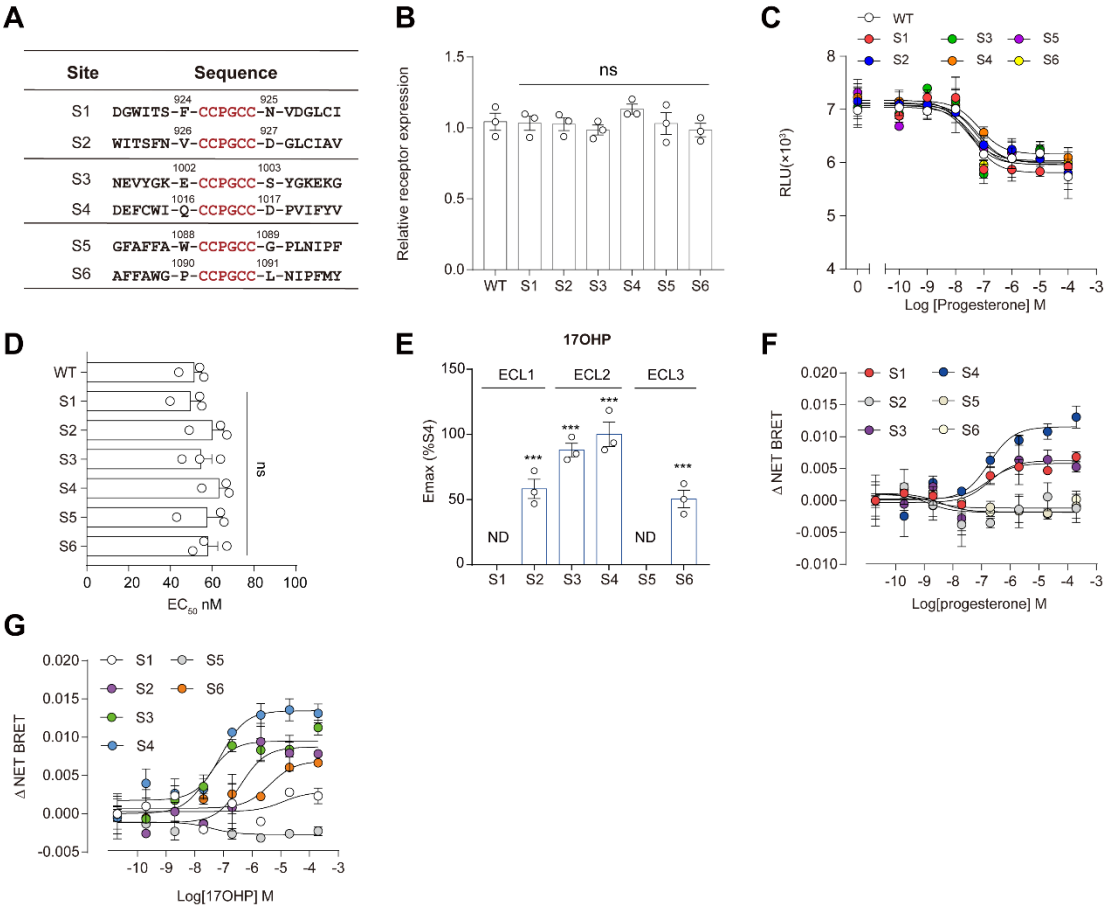

Supplemental Figure 5. Conformational changes within GPR126 extracellular domains as ligands binding.

A. Detailed description of the FlAsH motif (CCPGCC) incorporation site at the extracellular loops of GPR126. FlAsH motifs are labelled in red.

B. ELISA experiments to determine the expression levels of GPR126 wild-type (WT) and the indicated FlAsH-BRET mutants in HEK293 cells. Expression levels of indicated FlAsH-BRET mutants were compared to expression levels of wild-type GPR126. Data are shown as the mean ± SEM of three experiments (n=3) performed in triplicate. All data were statistically analyzed using one-way ANOVA with Tukey's test. ns, no significant difference.

C. Representative dose-response curves of progesterone and 17OHP induced cAMP inhibition in HEK293 cells over-expressing GPR126 wild-type (WT) and the indicated FlAsH-BRET mutants.

D. EC_{50} of curves in C were collected and presented in this graph. ns, no significant difference; the indicated FlAsH-BRET sensor was compared with GPR126 wild-type (WT). Data are

shown as the mean ± SEM of three experiments (n=3) performed in triplicate. All data were statistically analyzed using one-way ANOVA with Tukey's test. ns, not significant.

E. The maximal response of GPR126 FlAsH-BRET sensor S4 (annotated as WT) and the sensor-based CCPGCC mutants upon 17OHP stimulation. Data are derived from the dose-response curves in G, normalized to the maximal response of sensor S4. Values are the mean ± SEM from three independent experiments performed in triplicate. *** $p < 0.001$; ND, not detectable; FlAsH-BRET sensors stimulated with 17OHP were compared with those stimulated with control vehicle.

F and G. Representative dose-response curves of six GPR126 FlAsH-BRET sensors in response to progesterone (F) or 17OHP (G) stimulation.

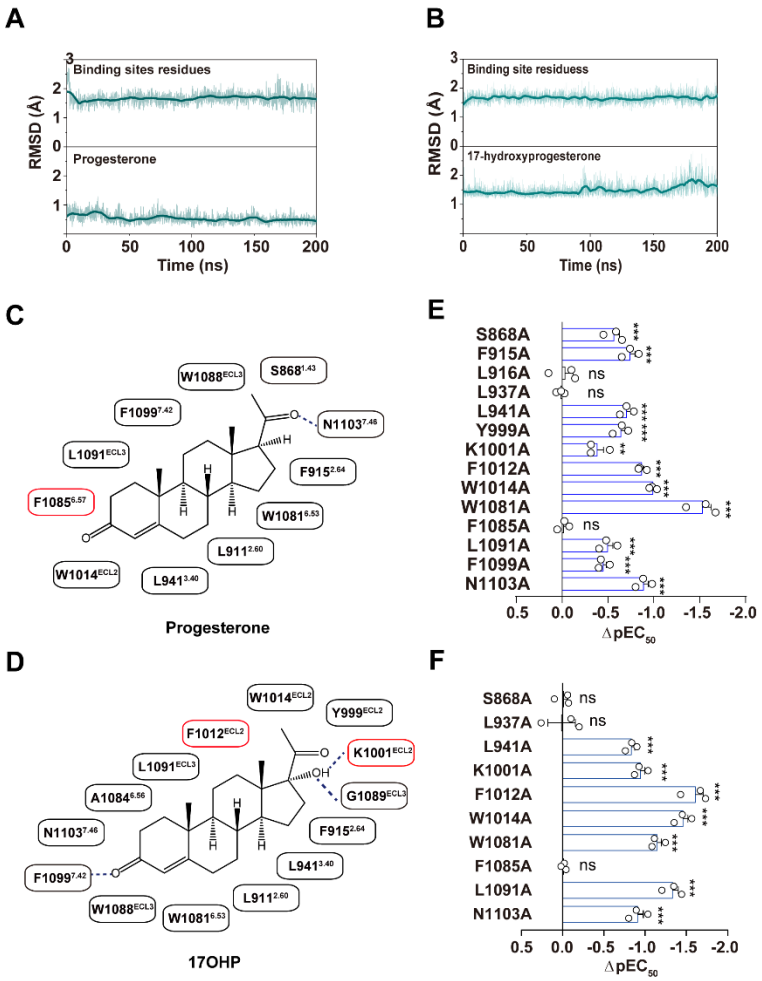

Supplemental Figure 6. Structural models of the interactions of progesterone and 17OHP within GPR126 ligand pocket.

A and B. RMSD analysis of progesterone-GPR126 (A) and 17OHP-GPR126 (B) during 200-ns molecular dynamics simulation trajectories by Gromacs. RMSDs of ligand (lower panel) or ligand binding pocket residues (upper panel) were showed in picture. The initial modeled complex state after equilibration (0 ns) was used for calculation.

C and D. Schematic diagram of interactions between progesterone and GPR126 residues as well as 17OHP and GPR126 residues. Hydrophobic stacking residues are shown with black box while residues referred to hydrogen bonds forming are shown with red box. Hydrogen bonds are depicted as red dashed lines.

E and F. Alanine mutagenesis scanning of putative residues in GPR126 ligand binding pocket on 17OHP-induced cAMP inhibition using GloSensor assay (E) or 17OHP-induced ECL2 conformational changes measured by FlAsH-BRET (F). Values are the mean ± SEM of three independent experiments. ** $p < 0.01$; *** $p < 0.001$; ns, no significant difference; GPR126-

WT transfected cells were compared to GPR126 mutant transfected cells. All data were analyzed by one-way ANOVA with Tukey's test. The ΔpEC50 values were obtained according to the data in Supplemental Figure 8A-8D and 8F-8H.

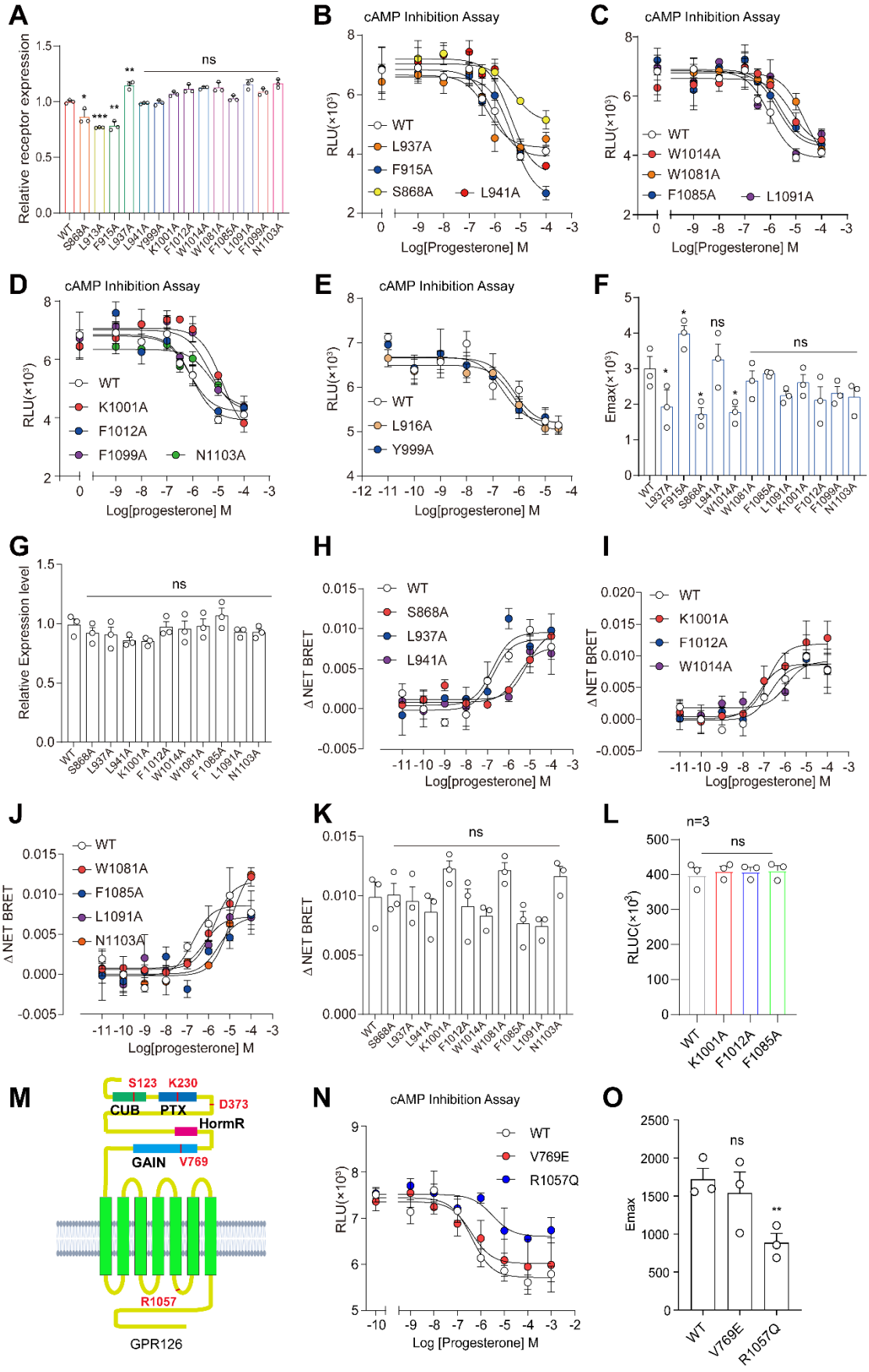
A
Relative receptor expression
ns
WT
S868A
L913A
F915A
L937A
L941A
Y999A
K1001A
F1012A
W1014A
W1081A
F1085A
L1091A
F1099A
N1103A
B
cAMP Inhibition Assay
RLU(×10³)
WT
L937A
F915A
S868A
L941A
Log[Progesterone] M
C
cAMP Inhibition Assay
RLU(×10³)
WT
W1014A
W1081A
F1085A
L1091A
Log[Progesterone] M
D
cAMP Inhibition Assay
RLU(×10³)
WT
K1001A
F1012A
F1099A
N1103A
Log[progesterone] M
E
cAMP Inhibition Assay
RLU(×10³)
WT
L916A
Y999A
Log[progesterone] M
F
Emax(×10³)
ns
G
Relative Expression level
ns
H
Δ NET BRET
WT
S868A
L937A
L941A
Log[progesterone] M
I
Δ NET BRET
WT
K1001A
F1012A
W1014A
Log[progesterone] M
J
Δ NET BRET
WT
W1081A
F1085A
L1091A
N1103A
Log[progesterone] M
K
Δ NET BRET
ns
L
n=3
ns
RLUC(×10³)
WT
K1001A
F1012A
F1085A
M
S123
K230
CUB
PTX
D373
HormR
GAIN
V769
R1057
GPR126
N
cAMP Inhibition Assay
RLU(×10³)
WT
V769E
R1057Q
Log [Progesterone] M
O
Emax
ns
WT
V769E
R1057Q

Supplemental Figure 7. Structural model for the interactions of progesterone with GPR126.

A. ELISA experiments to determine the expression levels of GPR126 wild-type (WT) and the indicated contacting residues mutants of GPR126 in HEK293 cells for GloSensor assay. Expression levels of indicated GPR126 mutants were compared to expression levels of wild-type GPR126. Data are shown as the mean ± SEM of three experiments (n=3) performed in triplicate. All data were statistically analyzed using one-way ANOVA with Tukey's test. ns, not significant, * $p < 0.05$, ** $p < 0.01$, *** $p < 0.001$.

B-E. Representative dose-response curves of cAMP inhibition in HEK293 cells overexpressing GPR126 wild-type (WT) or the indicated mutants of GPR126 stimulated by progesterone using GloSensor assay.

F. The efficacy changes upon progesterone activation for wild-type (WT) and mutant GPR126 corresponding to B-E. Emax of GPR126 mutants upon progesterone stimulation were compared to Emax of wild-type GPR126 after progesterone administration. Data are shown as the mean ± SEM of three experiments (n=3) performed in triplicate. All data were statistically analyzed using one-way ANOVA with Tukey's test. ns, not significant, * $p < 0.05$.

G. ELISA experiments to determine the expression levels of GPR126 wild-type (WT) and the indicated mutants in HEK293 cells for FlAsH-BRET assay.

H-J. Representative dose response curve of GPR126 FlAsH-BRET sensor S4 (annotated as WT) and the sensor-based alanine mutants in response to progesterone stimulation.

K. The BRET changes upon progesterone activation in H-J for sensor S4 (annotated as WT) and the sensor-based alanine mutants. BRET changes for sensor-based alanine mutants were compared to BRET changes for WT. Data are shown as the mean ± SEM of three experiments (n=3) performed in triplicate. All data were statistically analyzed using one-way ANOVA with Tukey's test. ns, not significant.

L. Basal BRET values were measured and analyzed for wild-type (WT) GPR126, K1001A, F1012A and F1085 mutants. The data were represented as the mean ± SEM from three independent experiments and Student's test was used for comparisons between two groups. Data in cells transfected with GPR126 mutants were compared to data in cells transfected with

wild-type (WT) GPR126. ns, not significant.

M. Locations of the indicated SNPs of GPR126 were indicated in schematic diagram.

N. Representative dose response curves of progesterone-stimulated cAMP inhibition in HEK293 cells over-expressing wild-type (WT) GPR126 or its mutants by Glosensor assay.

O. Emax values in N were collected and presented in this graph. ns, no statistical significance; Comparison between wild-type GPR126 and its mutants, Values are mean ± SEM from three independent experiments performed in triplicates. All data were analyzed by one-way ANOVA with Turkey test. ns, not significant, ** $p < 0.01$, *** $p < 0.001$.

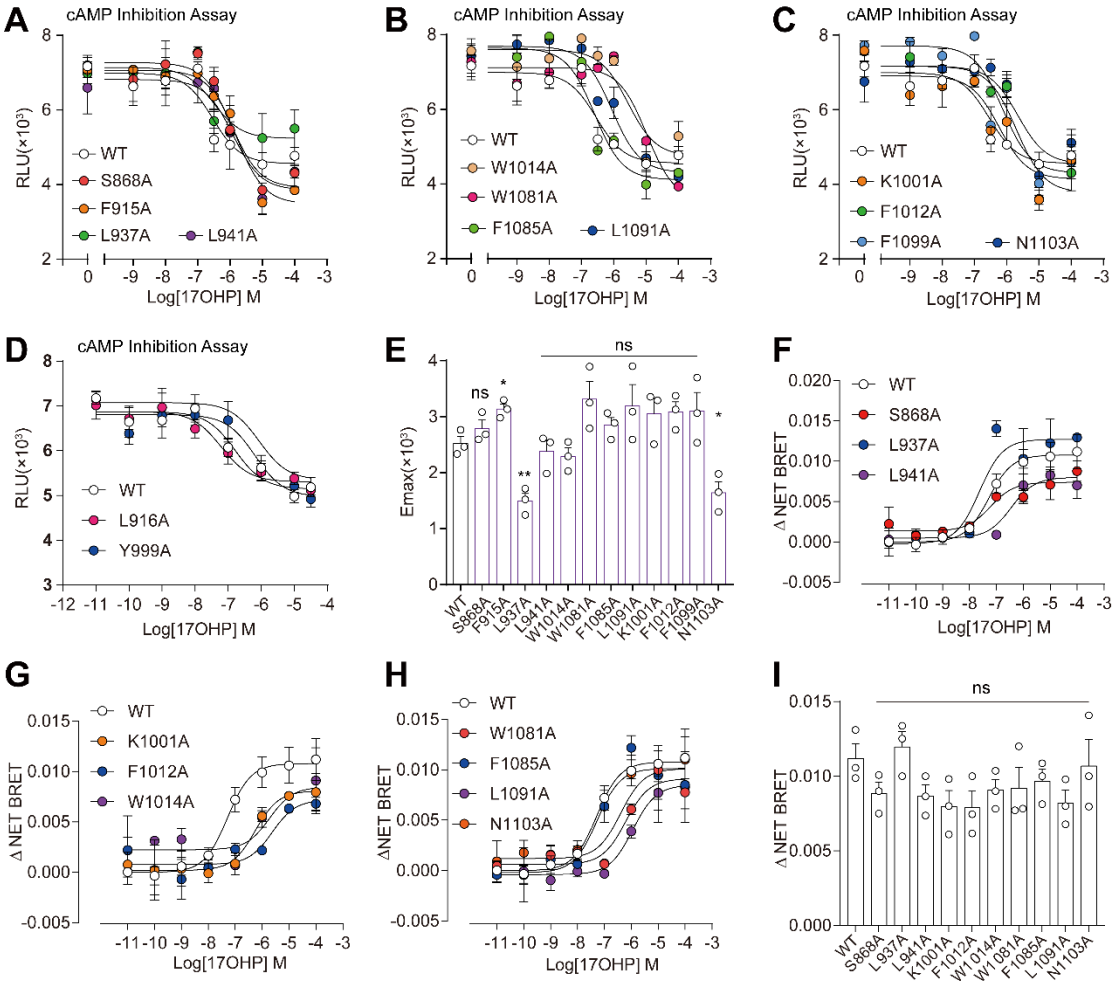

Supplemental Figure 8. Structural model for the interactions of 17OHP with GPR126

A-D. Representative dose-response curves of cAMP inhibition in HEK293 cells overexpressing wild-type (WT) GPR126 or the indicated mutants of GPR126 stimulated by 17OHP using GloSensor assay.

E. The efficacy changes upon 17OHP activation for wild-type (WT) and mutant GPR126 corresponding to A-D. Emax of GPR126 mutants upon 17OHP stimulation were compared to Emax of wild-type GPR126 (WT) after 17OHP administration. Data are shown as the mean ± SEM of three experiments (n=3) performed in triplicate. All data were statistically analyzed using one-way ANOVA with Tukey's test. ns, not significant, * $p < 0.05$, ** $p < 0.01$.

F-H. Representative dose response curves of GPR126 FlAsH-BRET sensor S4 (annotated as WT) and the sensor-based alanine mutants in response to 17OHP stimulation.

I. The BRET changes upon 17OHP activation in H-J for sensor S4 (annotated as WT) and the

sensor-based alanine mutants. BRET changes for sensor-based alanine mutants were compared to BRET changes for WT. Data are shown as the mean ± SEM of three experiments (n=3) performed in triplicate. All data were statistically analyzed using one-way ANOVA with Tukey's test. ns, not significant.

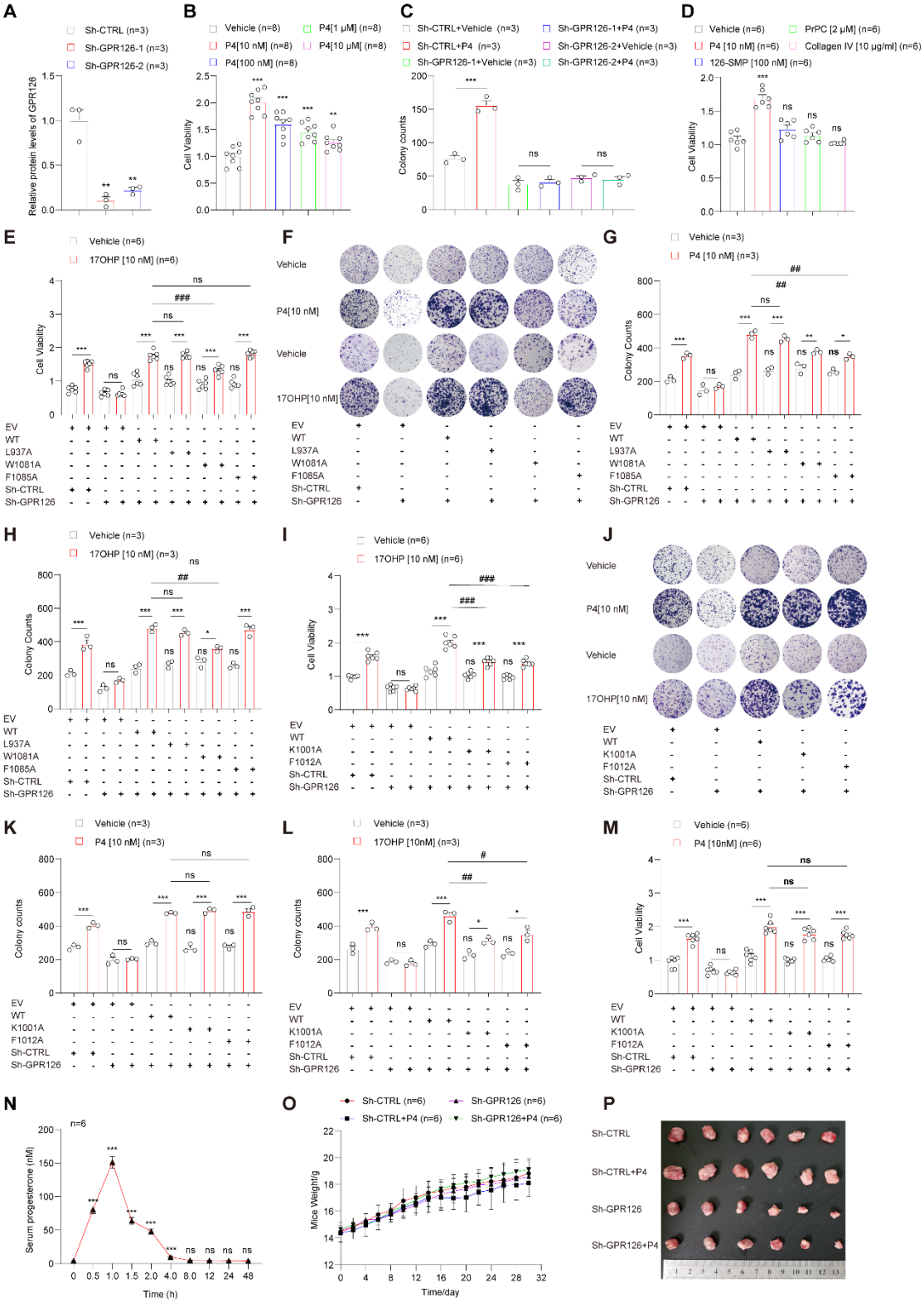

Supplemental Figure 9. Progesterone -triggered GPR126 activation promoted cell growth *in vitro* and tumorigenesis *in vivo*.

A. Quantification of the immunoblot bands in Figure 5A using Image J software. The data were represented as the mean ± SEM from three independent experiments and Student's test was

used for comparisons between two groups. Data in Sh-GPR126-1 or Sh-GPR126-2 cells were compared to data in Sh-CTRL cells. ** $p < 0.01$.

B. MDA-MB-231 cells were treated with the indicated concentrations of progesterone (P4, 10 nM) or DMSO (vehicle) for 72 h. Then cell proliferation was detected using MTT assay. The data were represented as the mean ± SEM from six independent experiments and Student's test was used for comparisons between two groups. Data in cells treated with different concentrations of P4 were compared to data in cells treated with vehicle. ** $p < 0.01$, *** $p < 0.001$.

C. MDA-MB-231 cells stably expressing sh-CTRL, sh-GPR126-1 or sh-GPR126-2 were treated with progesterone (P4, 10 nM) for 72h. Then cell proliferation was detected using colony formation assay. Colony numbers in P4 treated cells were compared to vehicle cells. Data are presented as the mean ± SEM from eight or three independent experiments and Student's test was used for comparisons between two groups. *** $p < 0.001$.

D. MDA-MB-231 cells were treated with the indicated ligands of GPR126 or DMSO (vehicle) for 72 h. Cell proliferation was analyzed by MTT assay. The data were represented as the mean ± SEM from six independent experiments and Student's test was used for comparisons between two groups. Data in cells treated with different ligands were compared to data in cells treated with vehicle. ns, not significant, *** $p < 0.001$.

E-H. MDA-MB-231 cells with stably GPR126 silencing (Sh-GPR126) were respectively transfected with wild-type (WT) GPR126, L937A, W1081A or F1085A mutants. Then cells were treated with progesterone (P4, 10 nM) or 17OHP (10 nM) for 72 h. Cell proliferation was analyzed by MTT assay (E) or colony formation assay (F) and colonies were counted and analyzed (G-H).

I. MDA-MB-231 cells with stably GPR126 silencing (Sh-GPR126) were respectively transfected with wild type GPR126 (WT), K1001A, F1012A, L937A, W1081A or F1085A mutants. Then the cells were treated with 17OHP (10 nM) for 72 h. Cell proliferation was analyzed by MTT assay. The data were represented as the mean ± SEM from six independent experiments and Student's test was used for comparisons between two groups. Data in cells treated with 17OHP were compared to data in cells treated with vehicle. ns, not significant, *** $p < 0.001$. Data in cells transfected with GPR126 mutants were compared to data in cells

transfected with WT. ns, not significant, ### $p < 0.001$.

J-M. MDA-MB-231 cells with stably GPR126 silencing (Sh-GPR126) were respectively transfected with wild-type (WT) GPR126, K1001A or F1012A mutants. Then cells were treated with progesterone (P4, 10 nM) or 17OHP (10 nM) for 72 h. Cell proliferation was analyzed by MTT assay (J) or colony formation assay (K) and colonies were counted and analyzed (L-M).

N-P. MDA-MB-231 cells (2×10^6 cells) that stably expressing sh-CTRL or sh-GPR126 were injected subcutaneously into the axilla of each nude mouse. Then, mice inoculated with sh-GPR126 or sh-CTRL cells were divided randomly into the following two groups that received either vehicle (DMSO) or progesterone (15 mg/kg) (n=6) via intraperitoneal injection. Serum progesterone levels were detected using ELISA Kit at different time points after progesterone injection (N). Mice weights were measured every 2 days (O). After 32 days, the nude mice were sacrificed. The dissected tumors are photographed (P) The data were represented as the mean ± SEM from six independent experiments and Student's test was used for comparisons between two groups. Progesterone levels at different time points were compared to progesterone levels at zero time point. ns, not significant, *** $p < 0.001$.

For E, G, H, K-M, the data were represented as the mean ± SEM from six independent experiments and Student's test was used for comparisons between two groups. Data in cells treated with progesterone (P4) or 17OHP were compared to data in cells treated with vehicle. ns, not significant, *** $p < 0.001$. Data in cells transfected with GPR126 mutants were compared to data in cells transfected with wild-type (WT) GPR126. ns, not significant, ## $p < 0.01$, ### $p < 0.001$.

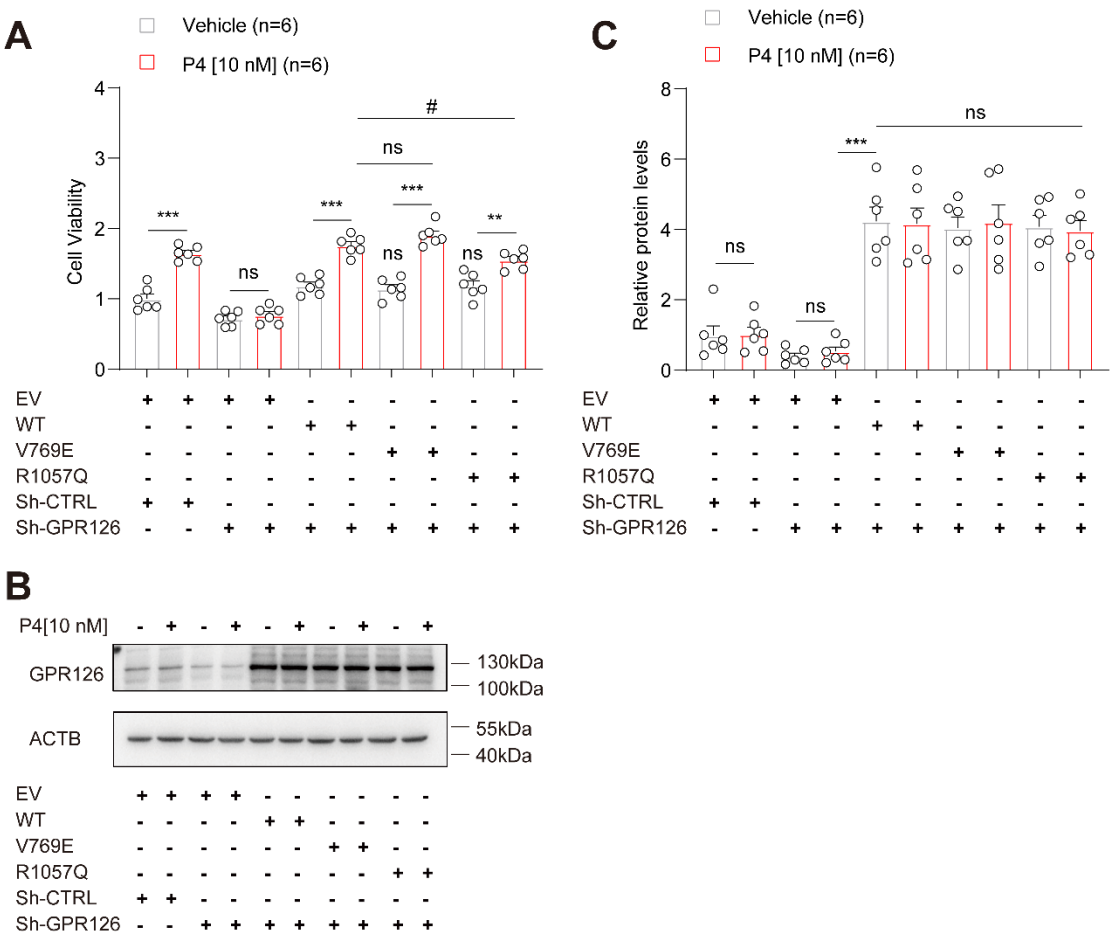

Fig 10. Effects of GPR126 SNPs on cell proliferation induced by progesterone.

MDA-MB-231 cells with stably GPR126 silencing (Sh-GPR126) were respectively transfected with wild-type (WT) GPR126, V769E or R1057Q mutants. Then the cells were treated with progesterone (P4, 10 nM) for 72 h. Cell proliferation was analyzed by MTT assay (A). GPR126 levels were analyzed by western blot (B) and the intensities of the immunoblot bands were quantified using Image J software (C). The data were represented as the mean ± SEM from six independent experiments and Student's test was used for comparisons between two groups. Data in cells treated with progesterone (P4) were compared with data in cells treated with vehicle. ns, not significant, ** $p < 0.01$, *** $p < 0.001$. Data in cells transfected with GPR126 mutants were compared to data in cells transfected with wild-type (WT) GPR126. ns, not significant, # $p < 0.05$.

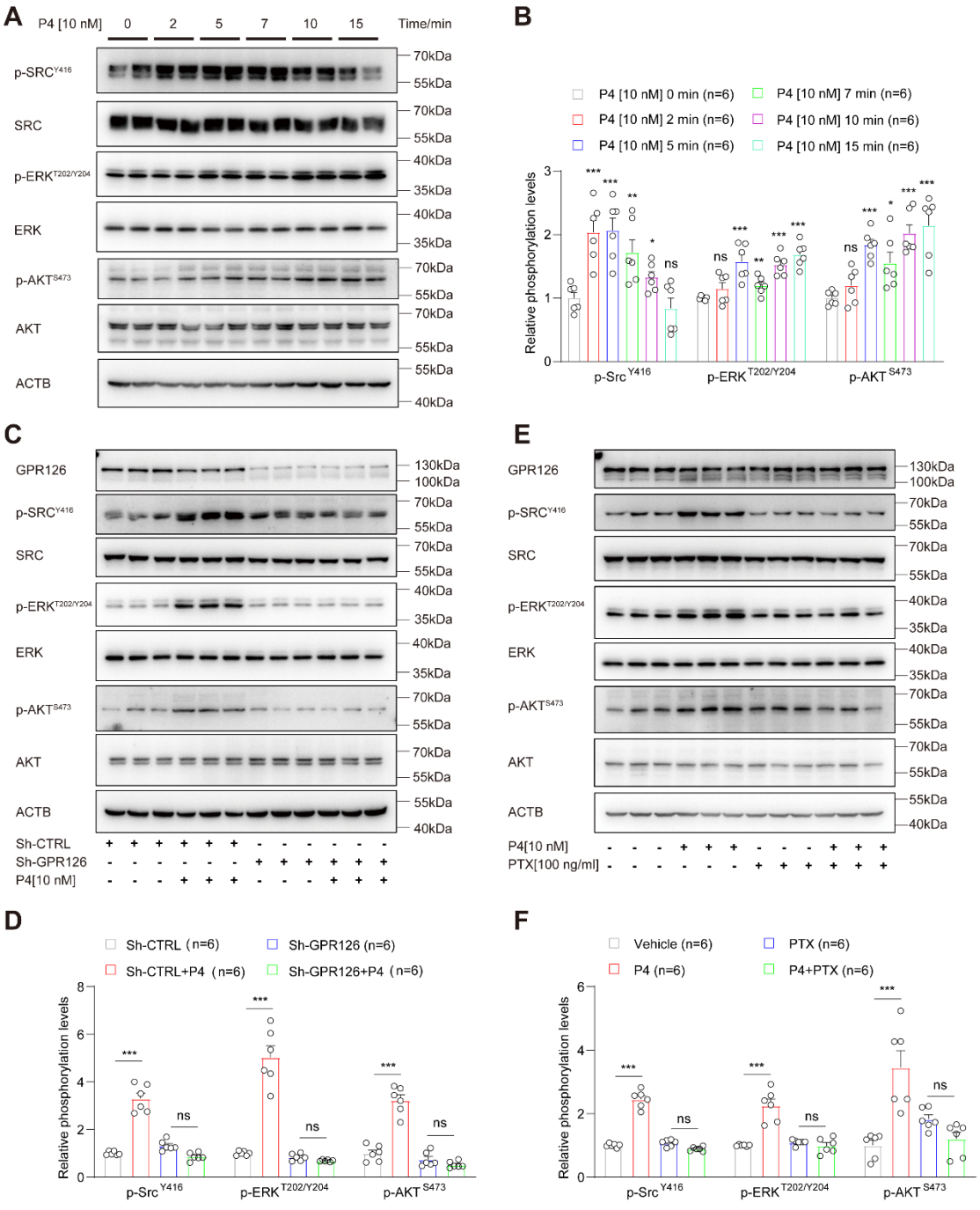

Supplemental Figure 11. Progesterone/GPR126-mediated cellular function is dependent on Gi-triggered SRC activation.

A-B. p-SRC^{Y416}, p-ERK$^{T202/Y204}$, p-AKT^{S473}and total SRC, ERK, AKT were detected by western blot in MDA-MB-231 cells treated with progesterone (10 nM) for the indicated time (A). The intensities of the immunoblot bands were quantified using Image J software (B). The data were represented as the mean ± SEM from three independent experiments and Student's test was used for comparisons between two groups. ns, not significant. * $p < 0.05$, ** $p < 0.01$, *** $p <$

0.001.

C. Western blot analysis of p-SRC^{Y416}, p-ERK$^{T202/Y204}$, p-AKT^{S473} in GPR126 stable silencing MDA-MB-231 cells (sh-GPR126) or their control cells (sh-CTRL treated with DMSO or progesterone (P4, 10 nM) for 5min, respectively.

D and F. Quantification of the immunoblot bands in C and E using Image J software. The data were represented as the mean ± SEM from six independent experiments and Student's t test was used for comparisons between two groups. ns, not significant. *** $p < 0.001$.

E. Western blot analysis of p-SRC^{Y416}, p-ERK$^{T202/Y204}$, p-AKT^{S473} in MDA-MB-231 cells treated with progesterone (P4, 10 nM) for 5min alone or in combination with PTX (100 ng/mL) for 16 h.

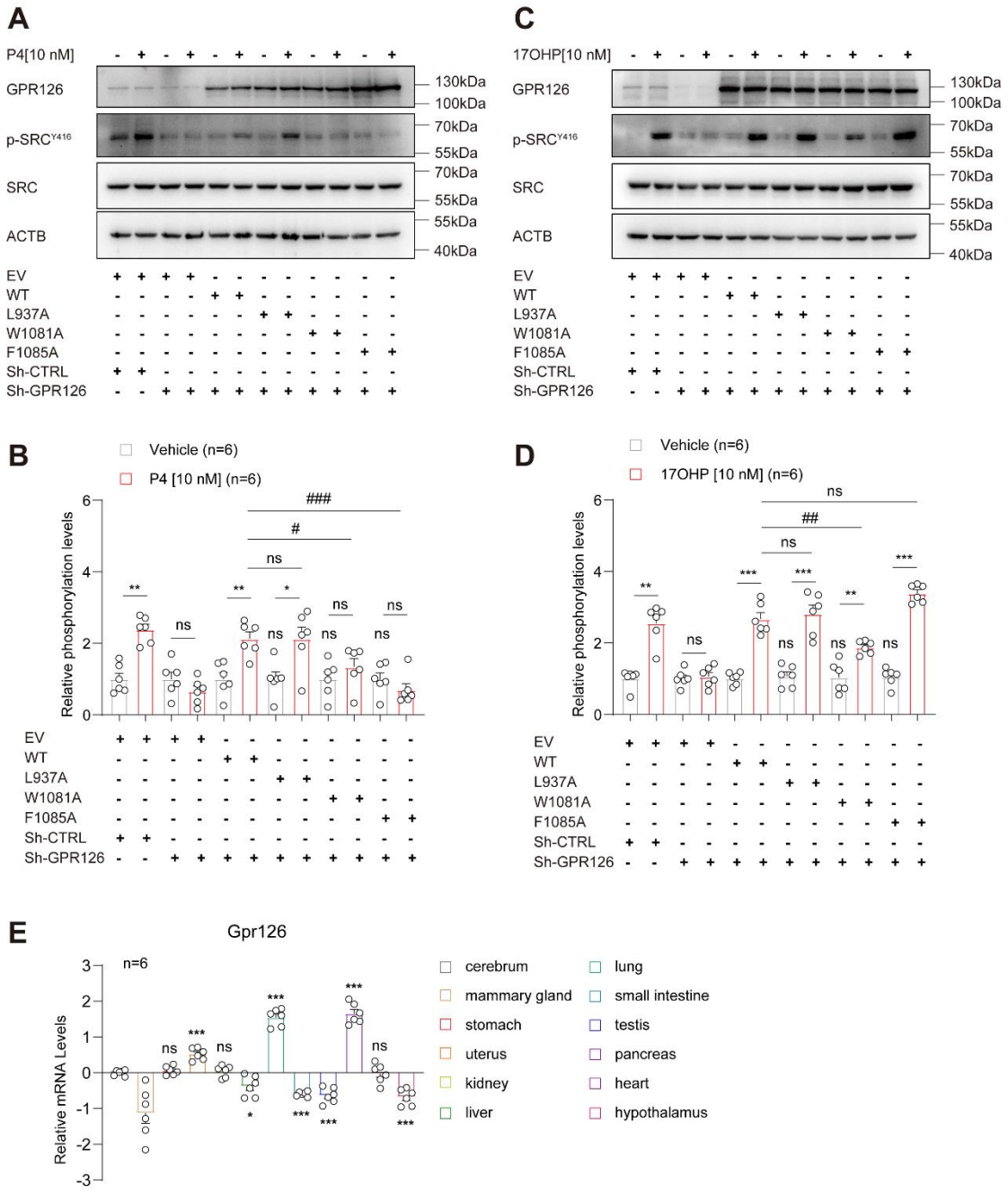

Supplemental Figure 12. Mutations in GPR126 affected phosphorylation of SRC in MDA-MB-231 cells induced by progesterone and 17OHP.

A and C. Western blot analysis of p-SRC^{Y416} in GPR126 silencing MDA-MB-231 cells (Sh-GPR126) with and overexpression of wild type GPR126 (WT), L937A, W1081A or F1085A mutants treated with progesterone (10 nM) (A) or 17OHP (10 nM) (C) for 5 min.

B and D. Quantification of the immunoblot bands in A and C using Image J software. The data were represented as the mean ± SEM from six independent experiments and Student's test was used for comparisons between two groups. Data in cells treated with progesterone (P4) or 17OHP were compared to data in cells treated with vehicle. ns, not significant, * $p < 0.05$, ** p

< 0.01, *** $p < 0.001$. Data in cells transfected with GPR126 mutants were compared to data in cells transfected with wild-type (WT) GPR126. ns, not significant, # $p < 0.05$, ## $p < 0.01$, ### $p < 0.001$.

E. Gpr126 mRNA levels were examined in different mice tissues. The data were represented as the mean ± SEM from six independent experiments and Student's test was used for comparisons between two groups. Gpr126 mRNA levels in other tissues were normalized and compared to that in cerebrum. ns, not significant, * $p < 0.05$, ** $p < 0.01$, *** $p < 0.001$.

Supplemental Table 1. GPR126 mutants primers

Name	Primers
GPR126-β-F	5’-CAAGGACGATGATGACAAAATGACTCATTTTGGGG-3’
GPR126-β-R	5’-GATCCATAAGCACCCCAAAATGAGTCATTTTGTCATC-3’
GPR126-β-ΔGPS-F	5’-CAAGGACGATGATGACAAAATGGACGCAAGGAATAC-3’
GPR126-β-ΔGPS-R	5’-CAGGACCTTAGTATTCCTTGCGTCCATTTTGTCATCATCG-3’
S868A-F	5’-CTAAGGTCCTGACATTTATTGCTTACATC-3’
S868A-R	5’-GCAGAAATTCCGCACCCGATGTAAGCAATAAATG-3’
F915A-F	5’-CTGCTGTTCCTCAATCTGCTGGCTCTGCTTG-3’
F915A-R	5’-GAAGTGATCCAGCCGTCAAGCAGAGCCAGCAG-3’
L916A-F	5’-GCTGTTCCTCAATCTGCTGTTTGCGCTTGACGGCTG-3’
L916A-R	5’-GAAGTGATCCAGCCGTCAAGCGCAAACAGCAG-3’
L937A-F	5’-GTGTATCGCTGTCGCGGTGCTGGCGCATTTTTTTC-3’
L937A-R	5’-GAATGTGGCCAGGAGAAAAAAATGCGCCAGC-3’
L941A-F	5’-CGCGGTGCTGCTGCATTTTTTTGCCCTGGC-3’
L941A-R	5’-CATCCAGGTGAATGTGGCCAGGGCAAAAAAATG-3’
Y999A-F	5’-GCAGAAATAACAACGAAGTGGCTGGAAAG-3’
Y999A-R	5’-CTTTCCCGTAGGACTCCTTTCCAGCCACTTC-3’
K1001A-F	5’-GAAATAACAACGAAGTGTATGGAGCGGAGTC-3’
K1001A-R	5’-CCTTCTCTTTCCCGTAGGACTCCGCTCCATAC-3’
F1012A-F	5’-GGGAAAGAGAAGGGGGATGAGGCCTGTTG-3’
F1012A-R	5’-CACGGGGTCCTGGATCCAACAGGCCTCATC-3’
W1014A-F	5’-GAGAAGGGGGATGAGTTCTGTGCGATCCAG-3’
W1014A-R	5’-GAAAATCACGGGGTCCTGGATCGCACAG-3’
W1081A-F	5’-GACATTTTTGCTGGGGATGACAGCGGGCTTC-3’
W1081A-R	5’-CCCAGGCAAAGAACGCGAAGCCCGCTGTC-3’
F1085A-F	5’-GGATGACATGGGGCTTCGCGGCCTTTGC-3’
F1085A-R	5’-GTTCAAGGGGCCCCAGGCAAAGGCCGCGAAG-3’
L1091A-F	5’-GTTCTTTGCCTGGGGCCCCGCGAACATC-3’

L1091A-R	5’-CAGGTACATGAAAGGGATGTTCGCGGGGC-3’
F1099A-F	5’-GAACATCCCTTTCATGTACCTGGCCAGTATATTC-3’
F1099A-R	5’-CTTGCAGGGAATTGAATATACTGGCCAGG-3’
N1103A-F	5’-CATGTACCTGTTCAGTATATTCGCTTCCC-3’
N1103A-R	5’-GAAAATAAACAGCCCTTGCAGGGAAGCGAATATAC-3’
S123G-F	5’-GGGCCTTAGCTTCAATAGTGGAGCTAATGAGATGCATG-3’
S123G-R	5’-GACACATGCATCTCATTAGCTCCACTATTGAAGC
K230Q-F	5’ -TTTTTGAGCATCTCCGATAGTCAGTGTCTTCTTAATAAC-3’
K230Q-R	5’-GCAAGGCGTTATTAAGAAGACACTGACTATCGGAGATGC-3’
D373E-F	5’-CAGAACTTGCGAGCTGTGCAGAACTGGGCACACTTTGTC-3’
D373E-R	5’-GCTTGACAAAGTGTGCCCAGTTCTGCACAGCTCGCAAG-3’
V769E-F	5’-GGAAGACACTCGTGAGCTACGAGATGGC-3’
V769E-R	5’-GATATTGCCGATACTGCAAGCCATCTCGTAGC-3’
R1057Q-F	5’-GGAACGGTAAAAGGTCTAATCAGACACTC-3’
R1057Q-R	5’-CGCAAAACTTCTTCTCTGAGTGTCTGATTAG-3’

Supplemental Table 2. GPR126 FlAsH mutants primers

Name	Primers
GPR126-Nluc-F1	5’-CAAGGACGATGATGACAAAATGGTCTTCACACTCGAAG-3’
GPR126-Nluc-R1	5’-CCTTAGTATTCCTTGCGTCGCTGCCTCCACCTCCACTCG-3’
GPR126-Nluc-F2	5’-GACGCAAGGAATACTAAGG-3’
GPR126-Nluc-R2	5’-GTCATCATCGTCCTTGTAG-3’
924F	5’-CTGTCCAGGTTGTTGCAACGTGGATGGTTTGTGTATCGCTG-3’
924R	5’-CTTGACGGCTGGATCACTTCATTTTGCTGTCCAGGTTGTTGC-3’
926F	5’-GTGTGCTGTCCAGGTTGTTGCGATGGTTTGTGTATCGCTGTC-3’
926R	5’-GCTGGATCACTTCATTTAACGTGTGCTGTCCAGGTTGTTGC-3’
1002F	5’-GTCCAGGTTGTTGCTCCTACGGGAAAGAGAAGGGGGATG-3’
1002R	5’-CGAAGTGTATGGAAAGGAGTGCTGTCCAGGTTGTTGCTCC-3’
1016F	5’-GTGCTGTCCAGGTTGTTGCGACCCCGTGATTTTCTATGTGAC-3’
1016R	5’-GATGAGTTCTGTTGGATCCAGTGCTGTCCAGGTTGTTGCG-3’
1089F	5’-GGTGCTGTCCAGGTTGTTGCGGCCCCTTGAACATCCCTTTC-3’
1089R	5’-GGGGCTTCGCGTTCTTTGCCTGGTGCTGTCCAGGTTGTTGC-3’
1091F	5’-CCTGCTGTCCAGGTTGTTGCTTGAACATCCCTTTCATGTACC-3’
1091R	5’-CTTCGCGTTCTTTGCCTGGGGCCCCTGCTGTCCAGGTTGTTG-3’